Innate Immunity Signaling: Cytosolic Ca^{2+} Elevation Is Linked to Downstream Nitric Oxide Generation through the Action of Calmodulin or a Calmodulin-Like Protein[1][W][OA]

Wei Ma, Andries Smigel, Yu-Chang Tsai, Janet Braam, and Gerald A. Berkowitz*

Agricultural Biotechnology Laboratory, University of Connecticut, Storrs, Connecticut 06269–4163 (W.M., A.S., G.A.B.); and Department of Biochemistry and Cell Biology, Rice University, Houston, Texas 77251 (Y.-C.T., J.B.)

Ca^{2+} rise and nitric oxide (NO) generation are essential early steps in plant innate immunity and initiate the hypersensitive response (HR) to avirulent pathogens. Previous work from this laboratory has demonstrated that a loss-of-function mutation of an Arabidopsis (*Arabidopsis thaliana*) plasma membrane Ca^{2+}-permeable inwardly conducting ion channel impairs HR and that this phenotype could be rescued by the application of a NO donor. At present, the mechanism linking cytosolic Ca^{2+} rise to NO generation during pathogen response signaling in plants is still unclear. Animal nitric oxide synthase (NOS) activation is Ca^{2+}/calmodulin (CaM) dependent. Here, we present biochemical and genetic evidence consistent with a similar regulatory mechanism in plants: a pathogen-induced Ca^{2+} signal leads to CaM and/or a CaM-like protein (CML) activation of NOS. In wild-type Arabidopsis plants, the use of a CaM antagonist prevents NO generation and the HR. Application of a CaM antagonist does not prevent pathogen-induced cytosolic Ca^{2+} elevation, excluding the possibility of CaM acting upstream from Ca^{2+}. The CaM antagonist and Ca^{2+} chelation abolish NO generation in wild-type Arabidopsis leaf protein extracts as well, suggesting that plant NOS activity is Ca^{2+}/CaM dependent in vitro. The CaM-like protein CML24 has been previously associated with NO-related phenotypes in Arabidopsis. Here, we find that innate immune response phenotypes (HR and [avirulent] pathogen-induced NO elevation in leaves) are inhibited in loss-of-function *cml24-4* mutant plants. Pathogen-associated molecular pattern-mediated NO generation in cells of *cml24-4* mutants is impaired as well. Our work suggests that the initial pathogen recognition signal of Ca^{2+} influx into the cytosol activates CaM and/or a CML, which then acts to induce downstream NO synthesis as intermediary steps in a pathogen perception signaling cascade, leading to innate immune responses, including the HR.

During their life cycle, plants must respond to the threat of invasion from numerous types of pathogenic microorganisms. The hypersensitive response (HR) is one component of the repertoire of plant innate immune defense reactions to avirulent pathogens that prevents the spread of the pathogen within the plant beyond the initial infection site. The HR, considered to be one type of programmed cell death (PCD; van Doorn and Woltering, 2005; Hofius et al., 2007), is characterized by the rapid death of cells in the local region surrounding an infection site. The death of the cells serves to limit the growth and development of the invading pathogen and to arrest the progress of disease symptoms caused by the pathogen (Dangl et al., 1996).

Plant innate immune signaling cascades involve cytosolic Ca^{2+} rise and nitric oxide (NO) generation, which ultimately lead to HR to avirulent pathogens (Dangl, 1998; Wendehenne et al., 2004; Delledonne, 2005; Lecourieux et al., 2006). Perception of a pathogen or conserved components of microbial cells (pathogen-associated molecular pattern [PAMP] molecules) induces Ca^{2+} influx across the plasma membrane, leading to cytosolic Ca^{2+} elevation as an early step in this signaling pathway (Lecourieux et al., 2002, 2006; Hu et al., 2004; Ali et al., 2007; Ma and Berkowitz, 2007). Arabidopsis (*Arabidopsis thaliana*) *defense, no death1* (*dnd1*) mutant plants lack a functional plasma membrane Ca^{2+}-conducting cyclic nucleotide-gated channel (CNGC2) and do not undergo HR (Clough et al., 2000; Ali et al., 2007). In wild-type Arabidopsis plants, application of the Ca^{2+} channel blocker Gd^{3+} can eliminate this inward Ca^{2+} current and prevent HR (Lemtiri-Chlieh and Berkowitz, 2004; Ali et al., 2007). Interestingly, overexpression of the chimeric gene *AtCNGC11/12* (this mutant CNGC may conduct Ca^{2+} constitutively

[1] This work was supported by the National Science Foundation (grant nos. 0721679 [to G.A.B.] and 0817976 [to J.B.]).

* Corresponding author; e-mail gerald.berkowitz@uconn.edu.

The author responsible for distribution of materials integral to the findings presented in this article in accordance with the policy described in the Instructions for Authors (www.plantphysiol.org) is: Gerald A. Berkowitz (gerald.berkowitz@uconn.edu).

[W] The online version of this article contains Web-only data.

[OA] Open Access articles can be viewed online without a subscription.

www.plantphysiol.org/cgi/doi/10.1104/pp.108.125104

in planta) in *Nicotiana benthamiana* leads to HR-like PCD in the absence of any avirulent pathogen (Yoshioka et al., 2006; Urquhart et al., 2007). AtCNGC11/12 was shown to conduct Ca^{2+}, and application of Ca^{2+} channel blockers abolished the *AtCNGC11/12*-induced PCD/HR (Urquhart et al., 2007). This evidence supports Ca^{2+} acting as an upstream signaling molecule in the cytosol that is necessary for HR.

At present, a wealth of information supports the essential role of NO in the plant HR response to avirulent pathogens (Dangl, 1998; Wendehenne et al., 2001, 2004; Romero-Puertas et al., 2004; Delledonne, 2005; Lamotte et al., 2005). Although NO generation in plants can occur from a number of different enzymatic and nonenzymatic pathways, NO generation contributing to HR development is due to Arg-dependent nitric oxide synthase (NOS) activity (Delledonne et al., 1998; Huang and Knopp, 1998; Zhang et al., 2003). For example, the application of a mammalian NOS inhibitor impairs HR in Arabidopsis and tobacco (*Nicotiana* spp.; Delledonne et al., 1998; Huang and Knopp, 1998). Inoculation with an avirulent pathogen elicits a NO burst in Arabidopsis leaf tissue (Zhang et al., 2003; Zeier et al., 2004), and this NO generation is blocked by a NOS inhibitor (Zhang et al., 2003).

It has been established that there is a connection between cytosolic Ca^{2+} elevation and NO synthesis during the plant innate immune response (Lamotte et al., 2004; Lecourieux et al., 2006; Ali et al., 2007). However, the mechanism by which Ca^{2+} rise is linked to NO generation is unknown. Application of the NO donor sodium nitroprusside to the Arabidopsis *dnd1* mutant (which lacks a Ca^{2+}-conducting channel, as discussed above) restores HR (Ali et al., 2007). The fungal PAMP cryptogein and the bacterial PAMP lipopolysaccharide (LPS) have been shown to elicit NO production in tobacco cell cultures (Lamotte et al., 2004) and Arabidopsis leaf cells (Zeidler et al., 2004; Ali et al., 2007); in both cases, application of a Ca^{2+} channel blocker or chelation of extracellular Ca^{2+} with EGTA prevented PAMP-induced NO generation.

Calmodulins (CaMs; seven genes) and CaM-like proteins (CMLs; 50 genes; McCormack and Braam, 2003) constitute a large family of potential Ca^{2+}-binding sensor proteins in Arabidopsis that may translate a signal of cytosolic Ca^{2+} elevation to downstream protein targets in numerous signal transduction cascades. Previous work (Heo et al., 1999; Chiasson et al., 2005; Takabatake et al., 2007) suggests that CaM (and/or a CML) is involved in plant pathogen signaling and the innate immune response. Constitutive expression of soybean (*Glycine max*) CaM (*SCaM-4* or *SCaM-5*) enhanced resistance to a broad spectrum of virulent and avirulent pathogens (Heo et al., 1999). Translational arrest of CaM *NtCaM13* results in tobacco plants that are more susceptible to fungal and bacterial pathogens (Takabatake et al., 2007). Reducing expression of the CML *APR134* in tomato (*Solanum lycopersicum*) depressed HR development (Chiasson et al., 2005). The mechanism mediating these CaM/CML-related plant responses to pathogens remains unresolved. Using intact guard cells of Arabidopsis leaf epidermal peels as a model system, we recently showed that the application of a CaM antagonist prevented Ca^{2+} channel- and NOS-mediated induction of NO by PAMPs, suggesting a link between Ca^{2+}, CaM, and NOS in the plant pathogen response signaling cascade (Ali et al., 2007).

In animal cells, the enzymatic activity of all three NOS isoforms requires Ca^{2+}/CaM as a cofactor (Nathan and Xie, 1994; Stuehr, 1999; Alderton et al., 2001; Crawford and Guo, 2005; Crawford, 2006). Importantly, animal NOS contains a CaM-binding domain (Stuehr, 1999). A NOS gene in plants has not yet been identified (Guo et al., 2003; Crawford et al., 2006; Zemojtel et al., 2006). It is unknown if, as is the case with animals, there is a pathogen-inducible NOS isoform in plants. In addition, the role of Ca^{2+}/CaM as an activator of NOS activity in any plant signaling cascade has not yet been demonstrated in planta beyond what can be inferred from our previous work (Ali et al., 2007). Here, biochemical and genetic evidence is presented indicating that cytosolic Ca^{2+} elevation during plant innate immunity signaling cascades could lead to NO generation through CaM/CML acting upstream from NO synthesis activation.

RESULTS

CaM Antagonist Effects on Pathogen Response Signaling and HR

HR development in Arabidopsis was evaluated by visual observation of necrosis (darkened areas) in ethanol-bleached leaves and ion leakage associated with PCD. Plants exposed to an avirulent pathogen (*Pseudomonas syringae* pv *tomato* DC3000 [*Pst*] *avrRpt2*$^+$) developed visually observable HR at a time point after inoculation when plants inoculated with a virulent pathogen (*Pst avrRpt2*$^-$) displayed no observable necrotic symptoms (see control leaves in Fig. 1A; Supplemental Fig. S1A). Coinfiltration of the CaM antagonist *N*-(6-aminohexyl)-5-chloro-1-naphthalenesulfonamide (W7) blocked HR development in response to *Pst avrRpt2*$^+$ (Fig. 1). Notably, the inactive W7 structural analog *N*-(6-aminohexyl)-1-naphthalenesulfonamide (W5) did not affect HR development (Fig. 1A). W7 and W5 had no observable effects on plants exposed to *Pst avrRpt2*$^-$ (Supplemental Fig. S1A).

NO synthesis (and possibly diffusion) in leaf tissue acts as a crucial and required signaling event leading to HR during the interaction between plants and avirulent pathogens (Zhang et al., 2003; Zeier et al., 2004; Ali et al., 2007). An Arg-dependent NOS-type enzyme mediates NO generation during this interaction (Zhang et al., 2003). Inhibition of NOS (Zhang et al., 2003) or abolishment of NO accumulation in the leaf (Zhang et al., 2003; Zeier et al., 2004) impairs HR to avirulent pathogens as well as other downstream and HR-associated outcomes such as the oxidative burst

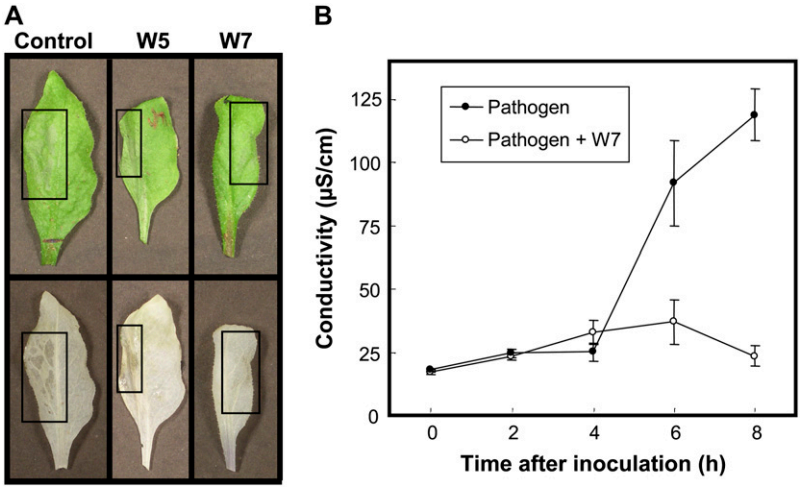

Figure 1. The CaM antagonist W7 prevents HR in wild-type plants. A, Inoculated regions of the leaves are highlighted by boxes. As shown in the top three panels, HR development becomes visible at 13 h after inoculation with *Pst avrRpt2*$^+$ pathogen alone (left) or with pathogen and W7 inactive analog W5 (center). However, HR is less evident in leaves inoculated with pathogen and 200 μM W7 (right). The bottom panels show the same leaves after ethanol bleaching for 4 d; HR development is evident as darkened regions. B, Measurement of ion leakage in leaves from a separate set of plants inoculated with (avirulent) pathogen or with pathogen and W7. Results are presented as means ± SE (n = 3).

(Zeier et al., 2004), indicating that NOS-mediated NO generation has an important function in this signal transduction cascade. In addition, NO has been suggested to act as a signal for cell-to-cell spread of HR (Zhang et al., 2003). NO generation during innate immune signaling has been monitored in planta using NO-specific fluorescent dyes (Zhang et al., 2003; Zeier et al., 2004). A NO scavenger, 2-(4-carboxyphenyl)-4,4,5,5-tetramethylimidazoline-1-oxyl-3-oxide potassium salt, blocked the NO-generated fluorescence induced by avirulent pathogen or a NO donor, indicating the specificity of the NO fluorescent dye in determining NO generation (Zhang et al., 2003). Here, we use a similar strategy to investigate the relationship between CaM and NO in this signal transduction cascade. As demonstrated by others (Zhang et al., 2003; Zeier et al., 2004), we detected NO generation induced by avirulent *Pst avrRpt2*$^+$ in leaves of wild-type Arabidopsis plants several hours after inoculation (Fig. 2A, left and center). Coinfiltration of the CaM antagonist W7 with pathogen impaired NO generation (Fig. 2A, center and right). Quantitative analysis of NO generation under the three aforementioned treatments is shown in Figure 2B. The results presented in Figures 1 and 2 are consistent with a model of pathogen signaling involving the activation of NO generation by a CaM or CML, and this NO generation is required for HR.

Prior work from this laboratory investigated the link between the inward Ca^{2+} current through the channel CNGC2, downstream NO generation, and HR (Ali et al., 2007). In this work, it was demonstrated that (1) a bacterial PAMP (LPS) activated inward Ca^{2+} current through channels formed by the CNGC2 translation product within minutes, (2) LPS application to cells evoked (external Ca^{2+}- and CNGC2-dependent) NO generation within minutes, (3) the CaM antagonist W7 blocked LPS-dependent NO generation, and (4) CNGC2-mediated Ca^{2+} conduction across plant cell membranes is required for plant HR to *Pst avrRpt2*$^+$. Here (as in Figs. 1 and 2), we evaluated the effects of W7 on this signaling pathway in planta. It is possible that W7 blocks HR and NO generation in the plant due to its effects on signaling from pathogen perception to the Ca^{2+} influx channel (influencing the early Ca^{2+} signal). Therefore, we tested this possibility as well.

Aequorin-transformed plants have been used to demonstrate cytosolic Ca^{2+} elevations in planta in response to pathogens and PAMPs (Grant et al., 2000; Lecourieux et al., 2002, 2005, 2006). As shown in Figure 3, we monitored the effect of W7 on pathogen-mediated cytosolic Ca^{2+} elevation in leaves of aequorin-expressing Arabidopsis plants. Inoculation of plants with pathogen (*Pst avrRpt2*$^+$) resulted in a cytosolic Ca^{2+} elevation initiated 5 to 10 min after inoculation that was not present in mock-inoculated control plants. The cytosolic Ca^{2+} elevation was still evident in plants coinfiltrated with pathogen and W7; this early (i.e. at 5–10 min) cytosolic Ca^{2+} elevation appears to be enhanced in the presence of W7. Grant et al. (2000) found a biphasic Ca^{2+} elevation in aequorin-expressing Arabidopsis plants inoculated with avirulent *Pst* and concluded that the second, sustained Ca^{2+} elevation that began 60 to 80 min after inoculation (and had a peak height above that of the first spike occurring 5–10 min after inoculation) was specifically associated with *avr* genes and therefore was associated with HR. Grant et al. (2000) presented results with *Pst* harboring the avirulence genes *avrRpm1* and *avrB*; here, we used *Pst avrRpt2*$^+$. In a number of experiments examining cytosolic Ca^{2+} elevation in response to *Pst avrRpt2*$^+$, we observed only a long sustained Ca^{2+} rise initiating approximately 45 min after inoculation, with a modest peak height lower than that of the first peak. Representative recordings over an extended period (3 h) in the presence and absence of W7 are shown in Supplemental Figure S2. W7 had no obvious inhibitory effect on the sustained Ca^{2+} rise. In a fashion similar to the results shown in Figure 3, the increase in the first (5–10 min) Ca^{2+} spike is evident in this experiment as well (Supplemental Fig. S2). The results shown in Supplemental Figure S2 indicate that over a long (3 h) time period, there is no evident inhibition in cytosolic Ca^{2+}

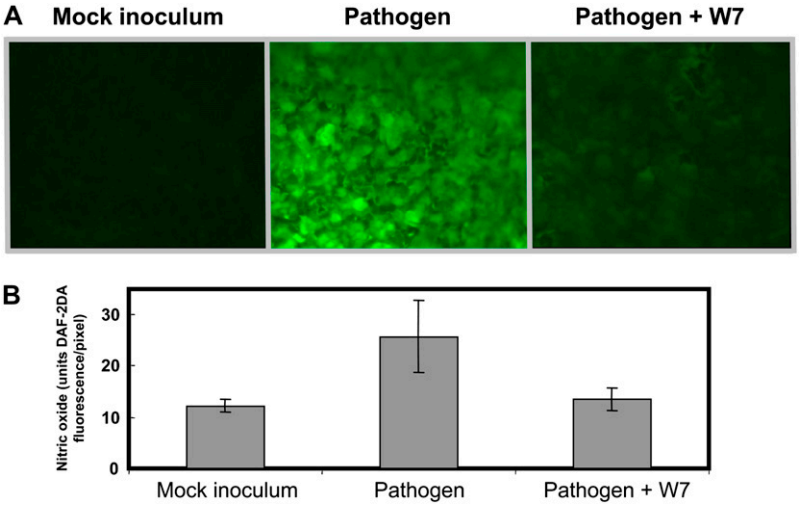

Figure 2. Coinfiltration of the CaM antagonist W7 impairs NO generation in wild-type leaves inoculated with avirulent pathogen *Pst avrRpt2*$^+$. A, NO generation was detected as fluorescence (green signal) within cells of wild-type leaves inoculated with mock inoculum, *Pst avrRpt2*$^+$, or *Pst avrRpt2*$^+$ and W7. Three leaves were evaluated per treatment; representative images are shown. B, Quantification of NO signal intensity in response to the treatments shown in A. Fluorescence of the entire area of each leaf captured in the camera field of view was quantified by measuring relative brightness within the defined range of 256 shades of gray per pixel (unit area). Results are presented as mean fluorescence intensity per pixel ± SE ($n = 3$). It should be noted that the NO binding fluorophore of DAF-2DA is generated only within cells upon cleavage of the ester linkage; hence, the dye responds only to intracellular NO. As the signal intensity of the entire leaf area within the field of view is quantified with the ImageJ software, the quantified signal per unit leaf area is an underestimation of the actual signal intensity within cells. Nonetheless, this analysis allowed for the quantification of treatment effects on NO generation. This experiment was repeated twice; results similar to those shown here were obtained in both experiments.

elevation occurring due to W7. Therefore, our finding that W7 blocks NO generation (Fig. 2) and HR (Fig. 1) in plants cannot be attributed to W7 effects on signaling from pathogen perception to the Ca^{2+} influx channel (Fig. 3; Supplemental Fig. S2).

Although we do not pursue the point in the work reported here, we suspect that the increase in pathogen-induced cytosolic Ca^{2+} elevation that occurs in the presence of W7 may be due to the effect of this CaM antagonist on CaM gating of CNGC channels mediating the Ca^{2+} influx. Previous work from this laboratory has already documented physical and functional interactions between plant CNGCs (including CNGC2) and several plant CaMs (Hua et al., 2003b; Ali et al., 2006). Moreover, it has been shown that CaM blocks inward CNGC cation currents (Hua et al., 2003a; Li et al., 2005; Ali et al., 2006). Recent patch clamp studies from this laboratory (Ali et al., 2007) indicated that sustained LPS-induced Ca^{2+} influx requires the presence of the CaM antagonist W7. The increase in the Ca^{2+} spike that occurs with W7 addition (Fig. 3) could be due to W7 antagonism of the CaM inhibition of a CNGC. Therefore, in the normal course of plant cellular response to pathogens, Ca^{2+}/CaM rise in the cytosol that would occur upon initial pathogen perception and early signaling could feed back to inhibit continued CNGC conduction (terminating the early Ca^{2+} influx signal by closing the CNGC) during the signaling cascade (Ma and Berkowitz, 2007). In any case, no decrease in pathogen-induced Ca^{2+} rise in the cytosol was found here in the presence of W7.

CML24 Acts Upstream from NO Generation during Plant Innate Immune Signaling

Chiasson et al. (2005) found that silencing the expression of a CML gene (*APR134*) in tomato suppressed HR; in their work, they did not identify which pathogen response signaling steps were impaired upon the loss of APR134 function. The Arabidopsis CaM-like protein CML24 has previously been shown to be involved in controlling NO accumulation (Tsai et al., 2007). CML24-regulated NO accumulation was

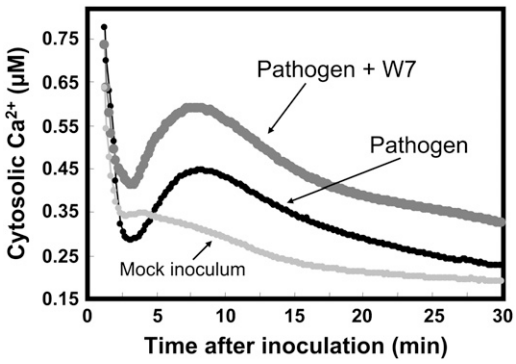

Figure 3. Application of the CaM antagonist W7 does not impair the cytosolic Ca^{2+} rise induced by *Pst avrRpt2*$^+$. Aequorin-expressing plants were infiltrated with avirulent pathogen (black line), pathogen coinfiltrated with the CaM antagonist W7 (200 μM; dark gray line), or a mock inoculum control (light gray line). This experiment was repeated three times with similar results.

shown to influence the timing of the transition to flowering (Tsai et al., 2007). Here, we investigated whether CML24 loss of function in *cml24-4* mutant Arabidopsis plants affected innate immune signaling. The *cml24-4* mutant shows an impaired HR to avirulent *Pst avrRpt2*$^+$ compared with wild-type plants (Fig. 4). In these experiments, we did not observe any HR-like necrosis development in wild-type or *cml24-4* mutant plants inoculated with virulent *Pst avrRpt2*$^-$ (Supplemental Fig. S1B). Evidence shown in Figure 4 demonstrates that CML24 is involved in plant innate immunity signaling, perhaps functioning as a sensor of the signal generated by Ca^{2+} influx to the cytosol (Fig. 3).

Next, we sought to determine whether CML24 has a role in NO accumulation during pathogen response. Recent work illustrates that Arabidopsis guard cells can be used as a model system to demonstrate NO signaling in plants (Guo et al., 2003; Melotto et al., 2006; Ali et al., 2007). LPS is a ubiquitous component of gram-negative bacteria, including *P. syringae* (Zeidler et al., 2004). LPS can elicit innate immune responses in both animals and plants, functioning as a PAMP (Nürnberger et al., 2004; Delledonne, 2005). PAMPs can induce NO generation in guard cells (Melotto et al., 2006; Ali et al., 2007) and epidermal and suspension cells (Zeidler et al., 2004). These studies, then, indicate that the application of LPS to guard cells is a useful tool for investigating pathogen-mediated NO signaling cascades. In prior work, we demonstrated, using several approaches, that LPS-mediated NO generation in guard cells of Arabidopsis epidermal peels requires Ca^{2+} influx into the cell and is inhibited by W7 (Ali et al., 2007). This work suggests Ca^{2+}/CaM (or a CML) involvement in signaling from pathogen perception to NO. Here, we extend this prior work by comparing LPS induction of NO generation in guard cells from wild-type and *cml24-4* mutant plants. As shown in Figure 5, NO generation in *cml24-4* guard cells treated with LPS is inhibited compared with wild-type cells. This result is consistent with the *cml24-4* impaired HR phenotype, suggesting that a disrupted NO generation response to the pathogen (or PAMP) could influence HR in this mutant.

We then examined in planta NO generation during HR signaling cascades and found that, in conjunction with the loss of HR to avirulent *Pst avrRpt2*$^+$ (Fig. 4), NO generation was also reduced in *cml24-4* mutant plants inoculated with the pathogen (Fig. 6). In summary, the results presented in Figures 4 to 6 provide genetic evidence complementing the studies with the CaM antagonist W7 (Figs. 1–3) linking CaM (or, in this case, a specific CaM-like protein, CML24) with NO generation and HR during pathogen response signaling transduction downstream from the initial cytosolic Ca^{2+} elevation.

CaM and Ca^{2+} Regulation of NOS Activity in Vitro

NO generation during pathogen signaling has been associated with increased NOS activity. CaM/CML induction of NO generation during pathogen signaling could be due to either direct or indirect activation of NOS-like activity. It is unknown if the plant enzyme responsible for Arg-dependent NOS-type NO generation has a CaM-binding domain (Zielinski, 1998). In addition, evidence has not been presented in the relevant literature that evaluates the possible Ca^{2+}/CaM dependence of NOS activity in plant tissue extracts. We undertook a series of experiments to address this hypothesis; results are shown in Figure 7.

Yamasaki and Sakihama (2000) have demonstrated that NaN_3 is a potent inhibitor of nitrate reductase (NR) activity (a potential enzymatic source of NO) in vitro. Here (Fig. 7A), we found no significant effect of NaN_3 on NO generation; the protein-dependent NO generation demonstrated in these extracts was not due to NR activity. NO generation in tissue extracts was reduced by the NOS inhibitor diphenyleneiodonium chloride (DPI) in our assay system (Fig. 7B), suggesting the presence of NOS-type activity. NO generation was reduced by 61% in the presence of DPI (Fig. 7B) and by 6% in the presence of NaN_3 (Fig. 7A).

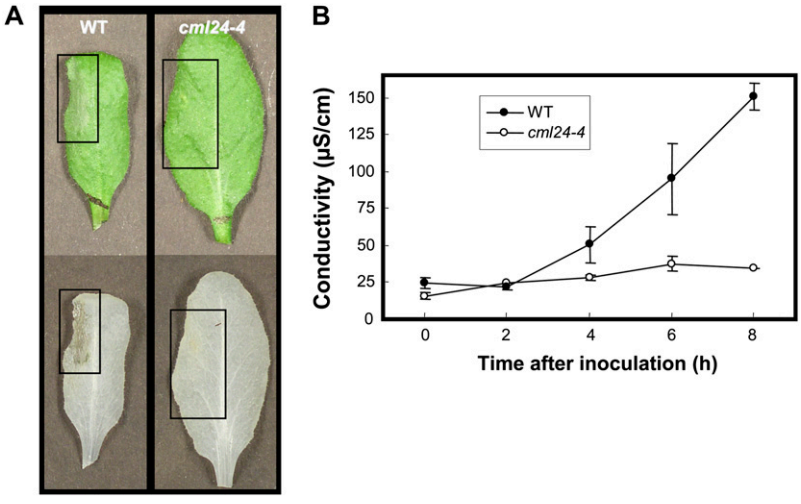

Figure 4. Loss-of-function *cml24-4* plants show an impaired HR phenotype. A, Inoculated areas of the leaves are highlighted by boxes. In the top two panels, HR development (17 h after inoculation with *Pst avrRpt2*$^+$) in wild-type (WT) and *cml24-4* leaves are shown at left and right, respectively. Leaves are shown after 4 d of ethanol bleaching in the bottom panels. This experiment was repeated four times with comparable results. B, Measurement of ion leakage in response to inoculation with *Pst avrRpt2*$^+$ using leaves from a separate set of plants. Results are presented as means ± SE (n = 3). This experiment was repeated two times.

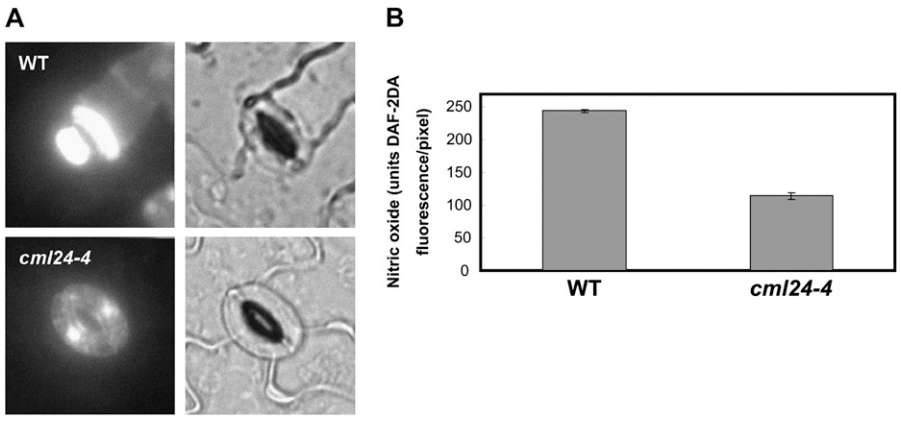

Figure 5. LPS-activated NO generation is disrupted in the *cml24-4* mutant. A, Fluorescence (left panels) and bright-field (right panels) images of guard cells in leaf epidermal peels from wild-type (WT) and *cml24-4* plants at a point of maximal fluorescence induced by LPS. B, Quantitative analysis of NO fluorescence signal recorded in wild-type and *cml24-4* guard cells, shown as mean fluorescence intensity per pixel ± SE ($n = 3$). This experiment was repeated three times.

Results of the experiment shown in Figure 7C indicate a clear Ca^{2+} dependence of this in vitro NOS activity when CaM is present in the assay. Removing free Ca^{2+} from the assay medium by the addition of a chelation agent (EGTA) reduced NO generation (by 75% at 1 mM EGTA). In the experiments shown in Figure 7, D and E, the effect of Ca^{2+} and CaM on NOS activity in the protein extracts was also evaluated. In the experiment shown in Figure 7D, NO generation was measured in the presence and absence of exogenous CaM and Ca^{2+}. The results indicate that leaving either CaM or Ca^{2+} out of the assay medium had a measurable, although modest, effect on NO generation. In this experiment, in the presence of CaM, adding Ca^{2+} increased NO generation (compare the white and gray bars in the left panel). In a corresponding fashion, in the presence of Ca^{2+}, adding CaM increased NO generation to a modest extent (compare the white bars in the left and right panels). The highest level of NO generation was obtained when both CaM and Ca^{2+} were present (i.e. a 48% increase over the level in the absence of both CaM and Ca^{2+}; compare the white bar in left panel with the gray bar in the right panel). This result suggests some level of dependence of this in vitro NOS activity on exogenously added Ca^{2+}/CaM. Even in the absence of added CaM, we found a modest (27%) increase in NO generation upon Ca^{2+} addition in this experiment (right panel). This result suggested the possibility that endogenous CaM may be present in the assay medium, perhaps physically associated with a NOS-type enzyme. CaM binds to one of the animal NOS isoforms (inducible NOS [iNOS]) very tightly (in a manner different from other animal NOS isoforms), even at basal levels of cellular Ca^{2+}. Even though Ca^{2+} (binding to the associated CaM) is required for maximal activity of iNOS (Spratt et al., 2007), CaM binds to iNOS effectively as soon as the protein is translated with such high affinity that CaM can be copurified during iNOS protein purification (Cho et al., 1992).

Based on this animal model, we speculated that the NOS protein apparently present in our tissue extracts could bind to CaMs (and/or CMLs) and, therefore, that our assay system could be influenced by endogenous CaM/CML associated with NOS. The results of the experiment shown in Figure 7E are consistent with this speculation. In the presence of exogenously added CaM, the addition of the CaM antagonist W7 had a strong inhibitory effect on NO generation (compare the white and gray bars in the left panel). However, in the absence of added CaM, the addition of W7 still had a substantial inhibitory effect on NO generation (right panel). We found similar effects as that shown in Figure 7E using another CaM antagonist, trifluoperazine dihydrochloride (data not shown). CaM antagonist inhibition of NO generation could occur if the effect was on endogenous CaM possibly present in the assay due to tight binding and association with NOS. Without the plant NOS enzyme "in hand," this point

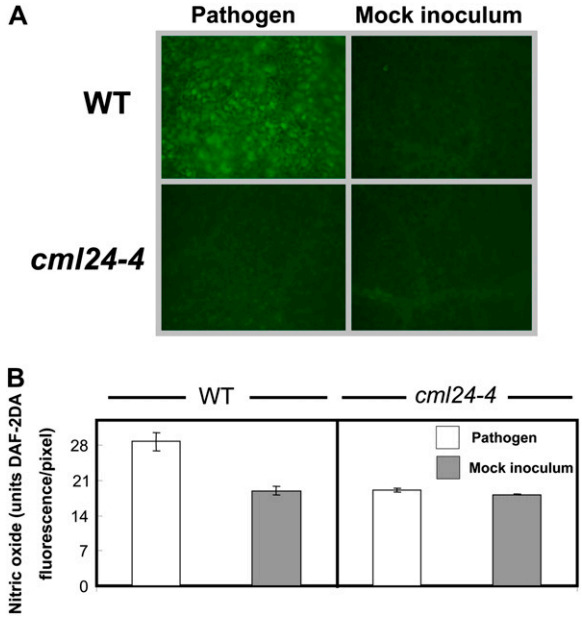

Figure 6. NO generation in leaves of wild-type (WT) and *cml24-4* plants inoculated with pathogen (*Pst avrRpt2*$^+$) or infiltrated with mock inoculum. As in Figure 2, images of leaf sections (A) or quantified fluorescence signal (B) are shown. For B, mean values of fluorescence intensity per pixel ± SE are shown ($n = 3$–4). This experiment was repeated twice.

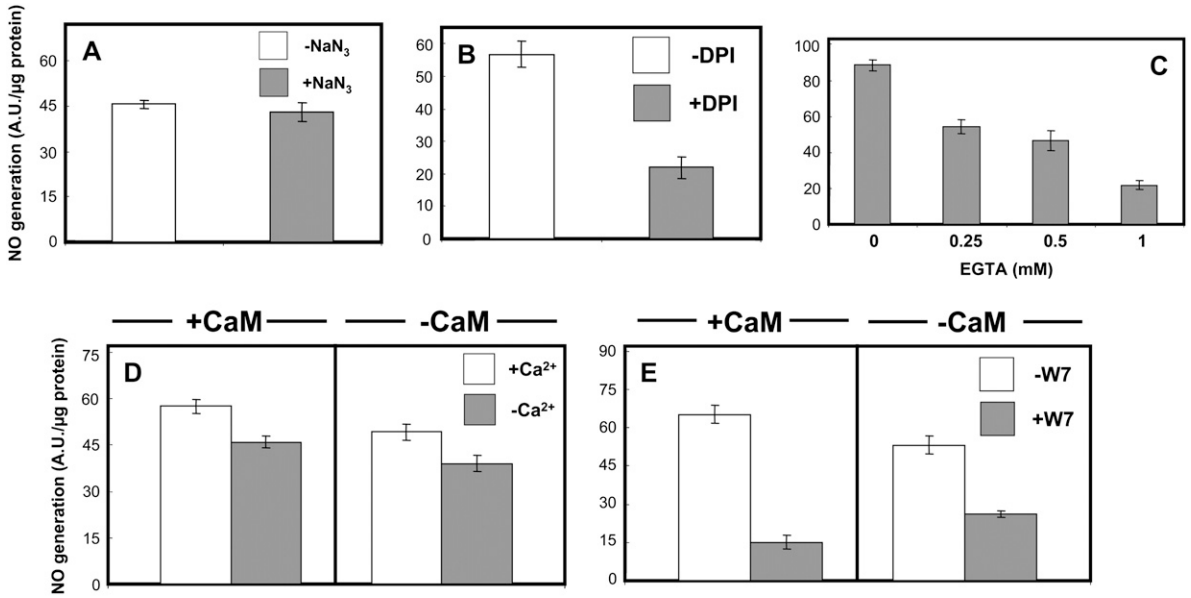

Figure 7. In vitro NO generation in crude protein extracts of leaves shows Ca^{2+}/CaM dependence. A, NO generation in the absence (white bar) and presence (gray bar) of the NR inhibitor (1 mM) NaN_3. B, NO generation in the absence (white bar) and presence (gray bar) of the NOS inhibitor (20 μM) DPI. C, Effect of the Ca^{2+} chelator EGTA on NO generation. D, All assays included 1 mM NaN_3. In the presence of this NR inhibitor, NO generation was monitored in the presence and absence of 1 mM Ca^{2+} and 1 μM CaM. E, In the presence (left) or absence (right) of 1 μM CaM, NO generation was monitored in the absence (white bars) or presence (gray bars) of 200 μM W7. All assays in A to C included 1 mM Ca^{2+} and 1 μM CaM. Assays in E included 1 mM Ca^{2+}. All results are presented as mean arbitrary fluorescence units ± SE ($n = 3$). Each experiment was repeated two to four times.

remains entirely speculative, albeit intriguing. Nonetheless, the results in Figure 7 suggest that NOS-dependent NO generation in cell-free Arabidopsis tissue extracts requires the Ca^{2+}/CaM complex for optimal activity. This finding is consistent with our interpretation of studies presented in this report regarding pathogen-related cellular Ca^{2+} elevation acting to induce NO generation and HR though CaM/CML effects on a putative NOS-type enzyme.

DISCUSSION

The evidence presented in this report is consistent with a model linking Ca^{2+} influx into the plant cell cytosol with NO generation during pathogen signaling cascades through the activation of NOS by Ca^{2+}/CaM or Ca^{2+}/CML complexes. Thus, this work provides some insight into molecular mechanisms that may underlie this component of plant innate immunity. However, we present this possible model with due caution. Most significantly, this model posits a direct interaction between CaM and NOS. Until the plant NOS gene is cloned or the protein purified and sequenced, clear and unequivocal evidence for the aforementioned model will be lacking. At this point, we can only tentatively conclude that cytosolic Ca^{2+} elevation activates NOS during innate immune responses through CaM or CML binding and activation of the enzyme directly responsible for NO generation during this plant signaling cascade. Perhaps CaM (or a CML) modulates an as-yet-unidentified protein acting upstream from NO generation. For example, AtNOS1/AtNOA1 (for Arabidopsis NITRIC OXIDE-ASSOCIATED PROTEIN1; formerly named AtNOS1) apparently acts upstream from NOS-mediated generation of NO; its mechanistic role in signaling leading to NO generation is unresolved, although it does not have a canonical CaM-binding domain (Guo et al., 2003; Crawford et al., 2006; Zemojtel et al., 2006). However, we demonstrate here a dependence of NOS activity in protein extracts on Ca^{2+} and CaM (Fig. 7), and it is difficult to envision the upstream proteins from NOS remaining associated with the downstream NO-generating step in our cell-free system. Thus, the most straightforward explanation for the work presented here remains the possible direct interaction/activation of NO generation by CaM/CML.

Another unresolved issue regarding our work is the protein interaction basis for the phenotypes of CML24 loss-of-function plants. It is apparent from the results shown in Figures 4 to 6 that loss of function of this specific CML affects NO signaling during innate immune responses, even though it could be expected that *cml24-4* mutant plants have many other functional CaM and CML proteins present in cells during pathogen response signaling. In some cases, it is thought that the temporal, spatial, and oscillatory aspects of a cytosolic Ca^{2+} elevation can impart a specific Ca^{2+} "signature" recognized by specific Ca^{2+}-responding proteins involved in signaling pathways (Batistic and Kudla, 2004). Within this context, there are other

examples in which the loss of function of one member of a large Ca^{2+}-responding protein family has affected the downstream Ca^{2+}-dependent response in plants (Cheong et al., 2007).

Another point of caution that should be considered when evaluating our proposed model regards our use of the CaM antagonists W7 and trifluoperazine dihydrochloride. These inhibitors bind to and act on proteins that, like CaMs and CMLs, contain paired helix-loop-helix Ca^{2+}-binding EF hands (Bouché et al., 2005); they are not specific inhibitors. Thus, they could also impair the function of calcineurin B-like proteins and Ca^{2+}-dependent kinases. A Ca^{2+}-dependent kinase was recently demonstrated to activate NADPH oxidase, an enzyme contributing to the oxidative burst and HR during plant innate immune responses (Kobayashi et al., 2007). However, the most straightforward explanation for the results shown in Figures 1 to 3 is an effect of the inhibitors on CaM/CML, acting downstream from the initial Ca^{2+} signal and upstream from NOS. Our use here of genetic approaches (the use of the *cml24-4* mutant) to complement the results we present with these inhibitors, as well as the results of our in vitro examination of CaM/NOS functional interactions, are consistent with the inhibitors acting to impair NOS activity through their antagonism of CaM/CML.

Finally, another important point relevant to the work presented here is that the model we propose does not preclude other factors from influencing the signaling cascade leading from pathogen perception through Ca^{2+} signaling to NO generation during plant innate immune responses. Clearly, this signal transduction system is complex and could involve many points of self-regulation as well as self-amplification (see reviews by Garcia-Brugger et al., 2006; Lecourieux et al., 2006; Ma and Berkowitz, 2007; Ma et al., 2007). Some evidence suggests that, in addition to an early Ca^{2+} signal promoting downstream NO and hydrogen peroxide generation during pathogen response signaling in plants, NO and hydrogen peroxide may activate plasma membrane Ca^{2+} conductance as well (Pei et al., 2000; Lamotte et al., 2004, 2006; Garcia-Brugger et al., 2006; Vandelle et al., 2006; Courtois et al., 2008). The identification here of CaM/CML as an intermediary step in the transduction of cytosolic Ca^{2+} elevation to NO generation, leading to HR, does not necessarily preclude an amplification and/or spread of the initial Ca^{2+} signal by these downstream molecules. Both NO and reactive oxygen species, as diffusible signaling molecules, have been envisioned to possibly act in pathogen response signaling pathways to spread the signal perception locally to neighboring cells (Levine et al., 1994; Zhang et al., 2003). In summary, we note that the pathogen response signaling cascade linking pathogen perception to NO generation and HR is complex, and clearly not all of the steps and protein components are yet identified. The work presented here does provide evidence indicating a possible mechanism linking cytosolic Ca^{2+} elevations to NO generation during this signal transduction system, in that CaM/CML antagonists were shown to affect pathogen-related NO generation and plant defense responses. In addition, the complementary genetic evidence presented here also supports this model.

MATERIALS AND METHODS

Plant Material

Arabidopsis (*Arabidopsis thaliana*) wild-type (Columbia ecotype), loss-of-function *cml24-4* mutant (Tsai et al., 2007), and aequorin-transformed (Grant et al., 2000) plants were grown in a growth chamber on LP5 potting mix containing starter fertilizer (Sun Gro) with 12 h of light (100 μmol m^{-2} s^{-1} illumination)/12 h of dark (72% relative humidity) and 22°C. The *cml24-4* genotype used in our studies was characterized in prior work (Tsai et al., 2007) as homozygous for a loss-of-function point mutation (E124K) in the CML24 (At5g37770) coding sequence (Tsai et al., 2007). In some cases, wild-type and *cml24-4* mutant plants were grown on top of potting mix covered with mesh for vacuum infiltration, as described by Katagiri et al. (2002). Typically, 6- to 8-week-old plants were used for all experiments. During growth, plants were irrigated with half-strength Murashige and Skoog solution (Caisson) two to three times to provide supplementary fertilizer. All chemicals were purchased from Sigma unless noted otherwise.

Pathogen Inoculation

All work in this report used the well-developed and much-studied pathogen-plant system of Arabidopsis exposed to the pathogen *Pseudomonas syringae* pv *tomato* DC3000 containing a specific avirulence gene (*Pst avrRpt2*). Experimental conditions (pathogen inoculum titer and postinoculation time period for necrosis evaluation) were selected that allowed for the development of HR symptoms by plants exposed to avirulent pathogen (*Pst avrRpt2*$^+$) at a point when plants exposed to virulent pathogen (*Pst avrRpt2*$^-$) displayed no observable necrotic symptoms (Supplemental Fig. S1). Avirulent (*avrRpt2*$^+$) and virulent (*avrRpt2*$^-$) strains of *Pst* were cultured in Luria-Bertani medium (Fisher Scientific) containing 50 μg mL^{-1} kanamycin (Fisher Scientific) and 20 μg mL^{-1} rifampicin (Fisher Scientific) overnight at 28°C, washed once in 10 mM $MgCl_2$ (Fisher Scientific), and resuspended typically at 1×10^7 colony-forming units (cfu) mL^{-1} in 10 mM $MgCl_2$. For the experiments shown in Figures 3 and 4A, bacterial resuspensions at 5×10^8 cfu mL^{-1} and 1×10^6 cfu mL^{-1} were used, respectively. For some experiments, interveinal regions of the abaxial surface of fully mature, nonsenescing leaves of plants (7 weeks old, grown in potting mix without mesh) were inoculated by delivery of bacterial suspensions to the intercellular subcuticular interior of the leaf with a 1-mL blunt-end syringe (Katagiri et al., 2002). Alternatively, vacuum infiltration was used to inoculate leaves (Katagiri et al., 2002). Plants (grown in pots with mesh) were submerged into solutions containing bacterial suspension in 10 mM $MgCl_2$ and the surfactant Silwet L-77 (Lehle Seeds) at 40 μL L^{-1} and then placed while submerged into a vacuum jar and subjected to negative pressure two to three times, each time for 1 min, until all of the leaves were fully infiltrated with the inoculum and appeared water soaked.

Evaluation of Tissue Necrosis and HR

For experiments using syringe inoculation of pathogen, leaves were detached from plants after inoculation (at the times after inoculation noted in the figure legends) and then soaked in ethanol for several days to remove pigments. Darkened areas of the bleached leaves corresponding to pathogen-induced tissue necrosis (Schornack et al., 2004; Weber et al., 2005; Ali et al., 2007) were used to evaluate HR development in response to pathogen infection. Alternatively, HR in pathogen-inoculated leaves was evaluated as ion leakage associated with PCD (Rate and Greenberg, 2001; Devadas and Raina, 2002; Torres et al., 2002). In this case, leaves from vacuum-infiltrated plants were used. Leaves were cut at the petiole (at the times after inoculation noted in the figure legends), and one leaf disc (0.7 cm diameter) was punched from each of four different detached leaves (four discs per replicate, three replicates per treatment in total). The four leaf discs per replicate were floated on 6 mL of deionized water (MilliQ water) at room temperature and shaken for 1 h with the abaxial surface of the leaf facing the water. Leaf discs were

then removed from the water, and conductivity was measured using an Orion 3 Star Benchtop Conductivity Meter (Thermo Scientific). For all experiments involving application of W7 or W5 (Calbiochem; 200 μM final concentration in aqueous solutions in all cases), stock solutions were made up in DMSO and control treatments included equivalent amounts of DMSO without W7 (or W5); the final concentration of DMSO was 0.4% (v/v).

In Vivo NO Analysis

LPS-dependent NO generation in guard cells of epidermal peels (Guo et al., 2003; Zeidler et al., 2004; Melotto et al., 2006) was monitored using the NO-specific fluorescent dye 4,5-diaminofluorescein diacetate (DAF-2DA) exactly as described by Ali et al. (2007). Epidermal peels were incubated in loading buffer (5 mM MES-KOH, 0.25 mM KCl, and 1 mM $CaCl_2$, pH 5.7) containing 50 μM DAF-2DA and then washed three times with buffer alone. After dye loading and washing, the peels were incubated for 5 to 10 min in Sigma NOS assay kit reaction buffer containing 100 μg mL^{-1} *Pseudomonas aeruginosa* phenol-extracted LPS. The epidermal peels were placed underneath a coverslip on a microscope slide with several drops of reaction buffer. NO-dependent DAF-2DA fluorescence was monitored over time; for each treatment, images show the maximum fluorescence intensity. NO-dependent DAF-2DA fluorescence and bright-field images were captured using an inverted Olympus IX70 microscope and GFP excitation and emission filters. Digitized images were acquired using a MagnaFire CCD camera and software. Quantitative analysis of the NO signal intensity in guard cell pairs was undertaken using ImageJ software as described by Ali et al. (2007) as well. The digitized image showing maximum fluorescence for guard cell pairs from an epidermal peel represented a genotype replicate; a minimum of three epidermal peels were analyzed as replicates for each genotype.

The method for NO detection in leaf tissue after pathogen inoculation was adapted from Zhang et al. (2003) and Zeier et al. (2004). After pathogen inoculation (or syringe injection of 10 mM $MgCl_2$ as a mock inoculation control), the inoculated region of the leaf was injected again 5.75 h later with 10 μM DAF-2DA dissolved in 10 mM Tris-KCl, pH 7.2 (Fisher Scientific). After this injection, plants were left in darkness for 30 min. NO generation in the inoculated leaf area was monitored as described above for epidermal peels using an inverted Olympus IX70 microscope with GFP excitation and emission filters. Digitized images were acquired using a MagnaFire CCD camera and software. NO signal intensity of the scanned entire field of the image captured by the digital camera was analyzed using ImageJ software.

In Vitro NO Generation in Leaf Protein Extracts

Protein was extracted from leaves of 8-week-old wild-type plants using a method adapted from Guo et al. (2003). Protein isolation was performed on ice. Nonsenescing rosette leaves (approximately 1 g) were mixed with 50 mg of polyvinylpolypyrrolidone and ground in liquid nitrogen. Powdered leaf tissue was resuspended in extraction buffer containing 50 mM Tris-HCl, pH 7.4, 320 mM Suc, 1 mM dithiothreitol, 1 mM phenylmethylsulfonyl fluoride, and commercial protease inhibitor cocktail (Roche Applied Science). Normally, 2 to 3 mL of extraction buffer was added to 1 g of powdered tissue. After vigorous shaking with a vortex, the homogenate was centrifuged at 4°C for 10 min (10,000*g*). The supernatant was transferred to a new centrifuge tube and spun again at 4°C for 30 min (15,000*g*). The supernatant was saved in aliquots, frozen in liquid nitrogen, and stored at −80°C. Protein concentration was measured using bicinchoninic acid protein assay reagent (Pierce) as described by Ma et al. (2006).

NO generation of leaf protein extracts was measured by monitoring DAF-2 fluorescence. A number of prior studies have used DAF-2 and analogs for measurement of NO generation in cell-free plant tissue and cell extracts (Yamasaki and Sakihama, 2000; Guo et al., 2003; Corpas et al., 2004; Zeier et al., 2004). Corpas et al. (2004) substantiated the efficacy of DAF-based dye use for the measurement of NO generation in cell-free systems by comparing this method with a number of other approaches for the quantification of NO in vitro. In addition to 10 μM DAF-2 (Calbiochem), the reaction mixture (100 μL) contained 45 mM Tris-HCl, pH 7.4, 1 mM L-Arg, 10 μM tetrahydrobiopterin, 10 μM FAD, 10 μM FMN, 1 mM β-NADPH, and leaf protein (approximately 2 μg). $CaCl_2$ (1 mM), commercial (bovine) CaM (1 μM), EGTA, DPI (20 μM), W7 (200 μM), or NaN_3 (1 mM; Fisher Scientific) was added as noted in the Figure 7 legend.

It should be noted that for these in vitro assays of Arg-dependent NO generation, we used the NOS inhibitor DPI rather than Arg analogs such as N_ω-nitro-L-Arg methyl ester or N_ω-nitro-L-Arg and N^G-methyl-L-Arg. These inactive Arg analogs have been commonly used to inhibit Arg-dependent NO generation in plant cells and leaves (Delledonne et al., 1998; Guo et al., 2003; Zhang et al., 2003; Zeidler et al., 2004; Ali et al., 2007). The presence of millimolar levels of Arg in our in vitro assay would confound any effects caused by the addition of these inactive Arg analogs. DPI, which inhibits NADPH-dependent flavoproteins, has been shown to inhibit purified animal NOS (Stuehr et al., 1991) as well as NOS-dependent NO generation in plants (Durner et al., 1998). DPI also inhibits the ROS-generating enzyme NADPH oxidase. However, our DAF fluorescence assay is not affected by ROS levels (Kojima et al., 1998). Furthermore, DAF has been shown to be unresponsive to DPI manipulation of ROS generation (Swindle et al., 2004). These prior studies support our use of DPI to probe for Arg-dependent NOS-type NO-generating activity in these in vitro experiments.

NO generation was monitored after incubation of the reaction mixture at 37°C for 1 h in darkness. The reaction mixture was added to wells of a 96-well microplate (black walls and clear bottom), and fluorescence signals were quantified using a FLUOstar Optima microplate reader (BMG Labtech) at excitation and emission wavelengths of 485 and 520 nm, respectively. Protein-dependent NO generation was ascertained by subtracting a background signal value from the individual treatment replicate values for an experiment. Background signal was typically obtained by measuring fluorescence signal in samples containing all reaction solution components (as detailed above) except protein. For later experiments, background values were ascertained in samples containing protein extraction buffer added to the NO fluorescence reaction solution. Our NO fluorescence assay was determined in control experiments to be linear at amounts below 8 μg of leaf protein; 2 μg was used in all work shown in this report.

Measurement of Pathogen-Induced Cytosolic Ca^{2+} Elevation in Aequorin-Expressing Plants

For these experiments, cytosolic Ca^{2+} elevation occurring in leaves inoculated with pathogen was evaluated using plants expressing cytosol-localized Ca^{2+}-dependent chemiluminescent aequorin protein. Homozygous Arabidopsis (Columbia ecotype) plants expressing apoaequorin under the control of the *35S* promoter as described by Grant et al. (2000) were used. Avirulent *Pst avrRpt2*$^+$ was grown on Luria-Bertani plates containing 2% agar, with similar levels of antibiotics as described above for liquid cultures. Bacteria were streaked onto plates and left in an incubator in the dark at 28°C for 24 to 36 h. Bacteria were taken from the outer, actively growing edge of the streaked colonies and diluted to 5×10^8 cfu mL^{-1} in 10 mM $MgCl_2$ (at room temperature). The bacterial solution was left at room temperature and immediately syringe injected into the abaxial side of Arabidopsis leaves containing the reconstituted aequorin protein (see below).

Apoaequorin-expressing Arabidopsis plants were grown in a growth chamber for 4 to 6 weeks before use. Coelenterazine-cp (CTZ-cp) was used to reconstitute aequorin. CTZ-cp was diluted to a stock concentration of 10 mM in methanol and then to a working concentration of 10 μM in ice-cold sterile MilliQ water. The CTZ-cp solution was syringe injected into the abaxial side of Arabidopsis leaves, under green light, until the entire leaf appeared to be water soaked. Plants were then placed into a light-proof box and incubated overnight at room temperature in complete darkness. CTZ-cp-injected leaves were used for luminescence readings as described below.

The luminescence of leaves inoculated with *Pst avrRpt2*$^+$ was monitored in whole leaves as photon emissions using a HIDEX Triathler liquid scintillation counter (Hidex Oy) with Commfiler I software for data capture. In a dark room under green light, leaves containing reconstituted aequorin were inoculated with bacterial suspension using a blunt-end syringe until the entire leaf appeared to be water soaked. The leaf was immediately detached from the plant and placed into a scintillation vial, and the sample was read for 30 min; luminescence readings were initiated within 10 to 15 s of inoculation. Luminescence counts were integrated every 10 s. Discharge of the remaining aequorin after luminescence measurements was done by adding 5 mL of 10% ethanol containing 1 mM $CaCl_2$ to the scintillation vial and taking additional luminescence readings for 1 h. Background was calculated using a non-transformed Columbia wild-type leaf, and the resulting value was subtracted from the luminescence readings at every time point. Quantification of aequorin remaining in leaves after the measurement period, and the background luminescence, were used to calculate cytosolic [Ca^{2+}] at 15-s intervals after inoculation as described by Allen et al. (1977). Leaves were inoculated with pathogen suspension with DMSO or W7 (in DMSO) as described above. The

effect of W7 was evaluated in three leaves, each from a different plant, and the Ca^{2+} signature shown is representative of three biological replications.

Supplemental Data

The following materials are available in the online version of this article.

Supplemental Figure S1. Virulent pathogen *Pst avrRpt2*$^-$ does not cause HR in Arabidopsis plants.

Supplemental Figure S2. Coinfiltration of the CaM antagonist W7 with avirulent *Pst avrRpt2*$^+$ does not affect the pathogen-associated long-term sustained cytosolic Ca^{2+} elevation.

Received June 22, 2008; accepted July 28, 2008; published August 8, 2008.

LITERATURE CITED

Alderton WK, Cooper CE, Knowles RG (2001) Nitric oxide synthases: structure, function and inhibition. Biochem J **357:** 593–615

Ali R, Ma W, Lemtiri-Chlieh F, Tsaltas D, Leng Q, von Bodman S, Berkowitz GA (2007) Death don't have no mercy and neither does calcium: *Arabidopsis* CYCLIC NUCLEOTIDE GATED CHANNEL2 and innate immunity. Plant Cell **19:** 1081–1095

Ali R, Zielinski R, Berkowitz GA (2006) Expression of plant cyclic nucleotide-gated cation channels in yeast. J Exp Bot **57:** 125–138

Allen DG, Blinks JR, Prendergast FG (1977) Aequorin luminescence: relation of light emission to calcium concentration: a calcium-independent component. Science **195:** 996–998

Batistic O, Kudla J (2004) Integration and channeling of calcium signaling through the CBL calcium sensor/CIPK protein kinase network. Planta **219:** 915–924

Bouché N, Yellin A, Snedden WA, Fromm H (2005) Plant-specific calmodulin-binding proteins. Annu Rev Plant Biol **56:** 435–466

Cheong YH, Pandey GK, Grant JJ, Batistic O, Li L, Kim BG, Lee SC, Kudla J, Luan S (2007) Two calcineurin B-like calcium sensors, interacting with protein kinase CIPK23, regulate leaf transpiration and root potassium uptake in Arabidopsis. Plant J **52:** 223–239

Chiasson D, Ekengren SK, Martin GB, Dobney SL, Snedden WA (2005) Calmodulin-like proteins from Arabidopsis and tomato are involved in host defense against *Pseudomonas syringae* pv. *tomato*. Plant Mol Biol **58:** 887–897

Cho HJ, Xie QW, Calaycay J, Mumford RA, Swiderek KM, Lee TD, Nathan C (1992) Calmodulin is a subunit of nitric oxide synthase from macrophages. J Exp Med **176:** 599–604

Clough SJ, Fengler KA, Yu IC, Lippok B, Smith RK Jr, Bent AF (2000) The Arabidopsis *dnd1* "defense, no death" gene encodes a mutated cyclic nucleotide-gated ion channel. Proc Natl Acad Sci USA **97:** 9323–9328

Corpas FJ, Barroso JB, Carreras A, Quirós M, León AM, Romero-Puertas MC, Esteban FJ, Valderrama R, Palma JM, Sandalio LM, et al (2004) Cellular and subcellular localization of endogenous NO in young and senescent pea plants. Plant Physiol **136:** 2722–2733

Courtois C, Besson A, Dahan J, Bourque S, Dobrowolska G, Pugin A, Wendehenne D (2008) Nitric oxide signalling in plants: interplays with Ca^{2+} and protein kinases. J Exp Bot **59:** 155–163

Crawford NM (2006) Mechanisms for nitric oxide synthesis in plants. J Exp Bot **57:** 471–478

Crawford NM, Galli M, Tischner R, Heimer YM, Okamoto M, Mack A (2006) Response to Zemojtel et al.: Plant nitric oxide synthase: back to square one. Trends Plant Sci **11:** 526–527

Crawford NM, Guo FQ (2005) New insights into nitric oxide metabolism and regulatory functions. Trends Plant Sci **10:** 195–200

Dangl JL (1998) Innate immunity: plants just say NO to pathogens. Nature **394:** 525–527

Dangl JL, Dietrich RA, Richberg MH (1996) Death don't have no mercy: cell death programs in plant–microbe interactions. Plant Cell **8:** 1793–1807

Delledonne M (2005) NO news is good news for plants. Curr Opin Plant Biol **8:** 390–396

Delledonne M, Xia Y, Dixon RA, Lamb C (1998) NO functions as a signal in plant disease resistance. Nature **394:** 585–588

Devadas SK, Raina R (2002) Preexisting systemic acquired resistance suppresses hypersensitive response-associated cell death in Arabidopsis hrl1 mutant. Plant Physiol **128:** 1234–1244

Durner J, Wendehenne D, Klessig DF (1998) Defense gene induction in tobacco by nitric oxide, cyclic GMP, and cyclic ADP-ribose. Proc Natl Acad Sci USA **95:** 10328–10333

Garcia-Brugger A, Lamotte O, Vandelle E, Bourque S, Lecourieux D, Poinssot B, Wendehenne D, Pugin A (2006) Early signaling events induced by elicitors of plant defenses. Mol Plant Microbe Interact **19:** 711–724

Grant M, Brown I, Adams S, Knight M, Ainslie A, Mansfield J (2000) The RPM1 plant disease resistance gene facilitates a rapid and sustained increase in cytosolic calcium that is necessary for the oxidative burst and hypersensitive cell death. Plant J **23:** 441–450

Guo FQ, Okamoto M, Crawford NM (2003) Identification of a plant NO synthase gene involved in hormonal signaling. Science **302:** 100–103

Heo WD, Lee SH, Kim MC, Kim JC, Chung WS, Chun HJ, Lee KJ, Park CY, Park HC, Choi JY, et al (1999) Involvement of specific calmodulin isoforms in salicylic acid-independent activation of plant disease resistance responses. Proc Natl Acad Sci USA **96:** 766–771

Hofius D, Tsitsigiannis DI, Jones JD, Mundy J (2007) Inducible cell death in plant immunity. Semin Cancer Biol **17:** 166–187

Hu XY, Neill SJ, Cai WM, Tang ZC (2004) Induction of defense gene expression by oligogalacturonic acid requires increases in both cytosolic calcium and hydrogen peroxide in Arabidopsis thaliana. Cell Res **14:** 234–240

Hua BG, Mercier RW, Leng Q, Berkowitz GA (2003a) Plants do it differently: a new basis for potassium/sodium selectivity in the pore of an ion channel. Plant Physiol **132:** 1353–1361

Hua BG, Mercier RW, Zielinski RE, Berkowitz GA (2003b) Functional interaction of calmodulin with a plant cyclic nucleotide gated cation channel. Plant Physiol Biochem **41:** 945–954

Huang JS, Knopp JA (1998) Involvement of nitric oxide in *Ralstonia solanacearum*-induced hypersensitive reaction in tobacco. *In* PH Prior, C Allen, JG Elphinstone, eds, Bacterial Wilt Disease: Molecular and Ecological Aspects. Springer-Verlag, Berlin, pp 218–224

Katagiri F, Thilmony R, He SY (2002) The *Arabidopsis thaliana-Pseudomonas syringae* interaction. *In* CR Somerville, EM Meyerowitz, eds, The Arabidopsis Book. American Society of Plant Biologists, Rockville, MD, doi/, http://www.aspb.org/publications/arabidopsis/

Kobayashi M, Ohura I, Kawakita K, Yokota N, Fujiwara M, Shimamoto K, Doke N, Yoshioka H (2007) Calcium-dependent protein kinases regulate the production of reactive oxygen species by potato NADPH oxidase. Plant Cell **19:** 1065–1080

Kojima H, Nakatsubo N, Kikuchi K, Kawahara S, Kirino Y, Nagoshi H, Hirata Y, Nagano T (1998) Detection and imaging of nitric oxide with novel fluorescent indicators: diaminofluoresceins. Anal Chem **70:** 2446–2453

Lamotte O, Courtois C, Barnavon L, Pugin A, Wendehenne D (2005) Nitric oxide in plants: the biosynthesis and cell signaling properties of a fascinating molecule. Planta **221:** 1–4

Lamotte O, Courtois C, Dobrowolska G, Besson A, Pugin A, Wendehenne D (2006) Mechanisms of nitric-oxide-induced increase of free cytosolic Ca^{2+} concentration in Nicotiana plumbaginifolia cells. Free Radic Biol Med **40:** 1369–1376

Lamotte O, Gould K, Lecourieux D, Sequeira-Legrand A, Lebrun-Garcia A, Durner J, Pugin A, Wendehenne D (2004) Analysis of nitric oxide signaling functions in tobacco cells challenged by the elicitor cryptogein. Plant Physiol **135:** 516–529

Lecourieux D, Lamotte O, Bourque S, Wendehenne D, Mazars C, Ranjeva R, Pugin A (2005) Proteinaceous and oligosaccharidic elicitors induce different calcium signatures in the nucleus of tobacco cells. Cell Calcium **38:** 527–538

Lecourieux D, Mazars C, Pauly N, Ranjeva R, Pugin A (2002) Analysis and effects of cytosolic free calcium increases in response to elicitors in *Nicotiana plumbaginifolia* cells. Plant Cell **14:** 2627–2641

Lecourieux D, Ranjeva R, Pugin A (2006) Calcium in plant defence-signalling pathways. New Phytol **171:** 249–269

Lemtiri-Chlieh F, Berkowitz GA (2004) Cyclic adenosine monophosphate regulates calcium channels in the plasma membrane of Arabidopsis leaf guard and mesophyll cells. J Biol Chem **279:** 35306–35312

Levine A, Tenhaken R, Dixon R, Lamb C (1994) H_2O_2 from the oxidative burst orchestrates the plant hypersensitive disease resistance response. Cell **79:** 583–593

Li XL, Borsics T, Harrington HM, Christopher DA (2005) Arabidopsis AtCNGC10 rescues potassium channel mutants of *E. coli*, yeast and Arabidopsis and is regulated by calcium/calmodulin and cyclic GMP in *E. coli*. Funct Plant Biol **32:** 643–653

Ma W, Ali R, Berkowitz GA (2006) Characterization of plant phenotypes associated with loss-of-function of AtCNGC1, a plant cyclic nucleotide gated cation channel. Plant Physiol Biochem **44:** 494–505

Ma W, Berkowitz GA (2007) The grateful dead: calcium and cell death in plant innate immunity. Cell Microbiol **9:** 2571–2585

Ma W, Yoshioka K, Berkowitz GA (2007) Cyclic nucleotide gated channels and Ca^{2+}-mediated signal transduction during plant innate immune response to pathogens. Plant Signal Behav **2:** 548–550

McCormack E, Braam J (2003) Calmodulins and related potential calcium sensors of Arabidopsis. New Phytol **159:** 585–598

Melotto M, Underwood W, Koczan J, Nomura K, He SY (2006) Plant stomata function in innate immunity against bacterial invasion. Cell **126:** 969–980

Nathan C, Xie QW (1994) Nitric oxide synthases: roles, tolls, and controls. Cell **78:** 915–918

Nürnberger T, Brunner F, Kemmerling B, Piater L (2004) Innate immunity in plants and animals: striking similarities and obvious differences. Immunol Rev **198:** 249–266

Pei ZM, Murata Y, Benning G, Thomine S, Klusener B, Allen GJ, Grill E, Schroeder JI (2000) Calcium channels activated by hydrogen peroxide mediate abscisic acid signalling in guard cells. Nature **406:** 731–734

Rate DN, Greenberg JT (2001) The *Arabidopsis aberrant growth and death2* mutant shows resistance to *Pseudomonas syringae* and reveals a role for NPR1 in suppressing hypersensitive cell death. Plant J **27:** 203–211

Romero-Puertas MC, Perazzolli M, Zago ED, Delledonne M (2004) Nitric oxide signaling functions in plant-pathogen interactions. Cell Microbiol **6:** 795–803

Schornack S, Ballvora A, Gurlebeck D, Peart J, Baulcombe D, Ganal M, Baker B, Bonas U, Lahaye T (2004) The tomato resistance protein Bs4 is a predicted non-nuclear TIR-NB-LRR protein that mediates defense responses to severely truncated derivatives of AvrBs4 and overexpressed AvrBs3. Plant J **37:** 46–60

Spratt DE, Taiakina V, Guillemette JG (2007) Calcium-deficient calmodulin binding and activation of neuronal and inducible nitric oxide synthases. Biochim Biophys Acta **1774:** 1351–1358

Stuehr DJ (1999) Mammalian nitric oxide synthases. Biochim Biophys Acta **1411:** 217–230

Stuehr DJ, Fasehun OA, Kwon NS, Gross SS, Gonzalez JA, Levi R, Nathan CF (1991) Inhibition of macrophage and endothelial cell nitric oxide synthase by diphenyleneiodonium and its analogs. FASEB J **5:** 98–103

Swindle EJ, Metcalfe DD, Coleman JW (2004) Rodent and human mast cells produce functionally significant intracellular reactive oxygen species but not nitric oxide. J Biol Chem **279:** 48751–48759

Takabatake R, Karita E, Seo S, Mitsuhara I, Kuchitsu K, Ohashi Y (2007) Pathogen-induced calmodulin isoforms in basal resistance against bacterial and fungal pathogens in tobacco. Plant Cell Physiol **48:** 414–423

Torres MA, Dangl JL, Jones JD (2002) Arabidopsis gp91phox homologues AtrbohD and AtrbohF are required for accumulation of reactive oxygen intermediates in the plant defense response. Proc Natl Acad Sci USA **99:** 517–522

Tsai YC, Delk NA, Chowdhury NI, Braam J (2007) Arabidopsis potential calcium sensors regulate nitric oxide levels and the transition to flowering. Plant Signal Behav **2:** 446–454

Urquhart W, Gunawardena AH, Moeder W, Ali R, Berkowitz GA, Yoshioka K (2007) The chimeric cyclic nucleotide-gated ion channel ATCNGC11/12 constitutively induces programmed cell death in a Ca^{2+} dependent manner. Plant Mol Biol **65:** 747–761

Vandelle E, Poinssot B, Wendehenne D, Bentéjac M, Pugin A (2006) Integrated signalling network involving calcium, nitric oxide, and active oxygen species but not mitogen-activated protein kinases in BcPG1-elicited grapevine defenses. Mol Plant Microbe Interact **19:** 429–440

van Doorn WG, Woltering EJ (2005) Many ways to exit? Cell death categories in plants. Trends Plant Sci **10:** 118–122

Weber E, Ojanen-Reuhs T, Huguet E, Hause G, Romantschuk M, Korhonen TK, Bonas U, Koebnik R (2005) The type III-dependent Hrp pilus is required for productive interaction of *Xanthomonas campestris* pv. *vesicatoria* with pepper host plants. J Bacteriol **187:** 2458–2468

Wendehenne D, Durner J, Klessig DF (2004) Nitric oxide: a new player in plant signalling and defense responses. Curr Opin Plant Biol **7:** 449–455

Wendehenne D, Pugin A, Klessig DF, Durner J (2001) Nitric oxide: comparative synthesis and signaling in animal and plant cells. Trends Plant Sci **6:** 177–183

Yamasaki H, Sakihama Y (2000) Simultaneous production of nitric oxide and peroxynitrite by plant nitrate reductase: in vitro evidence for the NR-dependent formation of active nitrogen species. FEBS Lett **468:** 89–92

Yoshioka K, Moeder W, Kang HG, Kachroo P, Masmoudi K, Berkowitz G, Klessig DF (2006) The chimeric *Arabidopsis* CYCLIC NUCLEOTIDE-GATED ION CHANNEL11/12 activates multiple pathogen resistance responses. Plant Cell **18:** 747–763

Zeidler D, Zähringer U, Gerber I, Dubery I, Hartung T, Bors W, Hutzler P, Durner J (2004) Innate immunity and Arabidopsis thaliana: lipopolysaccharides activate nitric oxide synthase (NOS) and induce defense genes. Proc Natl Acad Sci USA **101:** 15811–15816

Zeier J, Delledonne M, Mishina T, Severi E, Sonoda M, Lamb C (2004) Genetic elucidation of NO signaling in incompatible plant-pathogen interactions. Plant Physiol **136:** 2875–2886

Zemojtel T, Frohlich A, Palmieri MC, Kolanczyk M, Mikula I, Wyrwicz LS, Wanker EE, Mundlos S, Vingron M, Martasek P, et al (2006) Plant nitric oxide synthase: a never-ending story? Trends Plant Sci **11:** 524–525

Zhang C, Czymmek KJ, Shapiro AD (2003) NO does not trigger early programmed cell death events but may contribute to cell-to-cell signaling governing progression of the Arabidopsis hypersensitive response. Mol Plant Microbe Interact **16:** 962–972

Zielinski RE (1998) Calmodulin and calmodulin-binding proteins in plants. Annu Rev Plant Physiol Plant Mol Biol **49:** 697–725